PROCEEDINGS OF THE GEOLOGICAL SOCIETY OF CHINA
Vol.32, No.1, P.63-78, 11 Figs., January, 1989

GRAVITY SURVEY IN THE MINGHSIUNG-PEIKANG AREA, SOUTHWESTERN TAIWAN: POSSIBLE WESTWARD-EXTENSION OF THE MEISHAN FAULT

KUANG-JUNG CHEN, YIH-HSIUNG YEH,
CHENG-HORNG LIN, AND HORNG-YUAN YEN

Institute of Earth Sciences, Academia Sinica
P.O. Box 23-59, Taipei, Taiwan, R.O.C.

ABSTRACT

A detailed gravity survey has been carried out in the Minghsiung-Peikang area, southwestern Taiwan. This survey covers an area of about 260 km^2 . The Bouguer anomaly map is relatively simple. Except for some closed gravity low areas near Hsinkang, most contours of the map trend in the NNW-SSE direction. The anomaly more or less decreases gradually from the WSW to the ENE. This implies that the strata in this area is likely to dip to the northeast. The distribution patterns of residual and second derivative Bouguer anomalies show some specific characteristics which indicate the possibility of the westward extension of the Meishan fault from Minghsiung. Four profiles of subsurface structures in the study area have been modeled. The results show that the Meishan fault may extend westward at least 6 km from Minghsiung. The dip angle of the extension part of this fault is about 60 to 80 and the throw varies from 50 meters to 200 meters. In addition, several local normal faults exist in the study area. We suggest that they might be associated with the Meishan fault.

INTRODUCTION

A major earthquake of M_L 7.1, whose focal depth was determined to be very shallow (Hsu, 1980), occurred near Meishan on March 17, 1906. This event and a series of strong aftershocks killed 1266 people, injured 2476 persons, destroyed 7284 and damaged a further 30,021 houses (Omori, 1907). The Meishan fault was associated with this earthquake with a maximum vertical displacement of 180 cm and a maximum horizontal displacement of 240 cm in Kaiyenho (Omori, 1907). This fault trends S75°W over most of its length. But toward its western end it turns S53°W and then extends nearly

due west to Minghsiung. The straight-line distance between the mapped ends of this fault is about 13 km. According to the surface geology surveys, there was no obvious trace of fault west of Minghsiung (Omori,1907). However, large quantities of sand and water from fissures flowed out which extended 12 km west of Minghsiung. Omori inferred that the meishan fault might extend a further 12 km to the west. Based on the hinge character of the Meishan fault observed near Kaiyenho, Omori believed that the Meishan fault might extend 25 km to the east. Thus, the length of the Meishan fault may be 50 km in total.

Since it is very important for the mitigation of earthquake hazards in the Chiayi-Tainan area to know the reality and extent of the westward extension of the Meishan fault, a detailed gravity survey is used in this study to delineate the westward extension in this study. The gravity survey was carried out by a LaCoste-Romberg microgal gravimeter in the Minghsiung-Peikang area. Bouguer, residual, and second derivative anomalies are used to infer the possibility of the westward extension of the Meishan fault. In addition, modeling of subsurface structures along four profiles are also made.

GEOLOGY REVIEW

Many geologists have done the surface geology surveys in the Minghsiung-Peikang area (Chang,1963, 1964; Ho, 1975; Kuan, 1983). Fig. 1 shows a simplified version of the geologic map of this area. The area is covered primarily by alluvium and laterite deposits. Its surface geology is quite monotonous. Only the Liushuang Formation and the Erhchungchi Formation of Plio-Pleistocene age are exposed locally to the east of Minghsiung. Other formations such as the Kanhsialiao Formation, Liuchungchi Formation, and Yungshuichi Formation of Pliocene age do not outcrop in this area. The Liushuang Formation is about 1040 m thick, composed mostly of dark gray to bluish gray mudstone and shale with thin sand and silt interbeds. This formation is equivalent to the Houyenshan facies of the Toukoushan Formation in northern Taiwan. The Erchungchi Formation is composed of alternating beds of shale and fine- to medium-grained sandstone. Its thickness in the type section is approximately 440 m. The Kanhsialiao Formation, which is 540 m thick at the type locality, is composed mainly of shale with some sandstone interbeds. The Liuchungchi Formation is composed mainly of dark gray, fine-grained, muddy sandstone and sandy shale intercalated with shale and sandstone. Its thickness is about 760 m in the type section. The Yungshuichi Formation is about 450 m thick at the type locality. This formation is divided into three members: the upper and middle members are equivalent to the Cholan Formation, and the lower member is equivalent to the Chinshui Shale. The formation is composed of shale and sandy shale with muddy sandstone interbeds and reef limestone lenses.

The major geologic structures in this area (Fig. 1) consist of fault "A", fault "B", and the Meishan fault. Fault "A" , also called the "Yichu Marginal

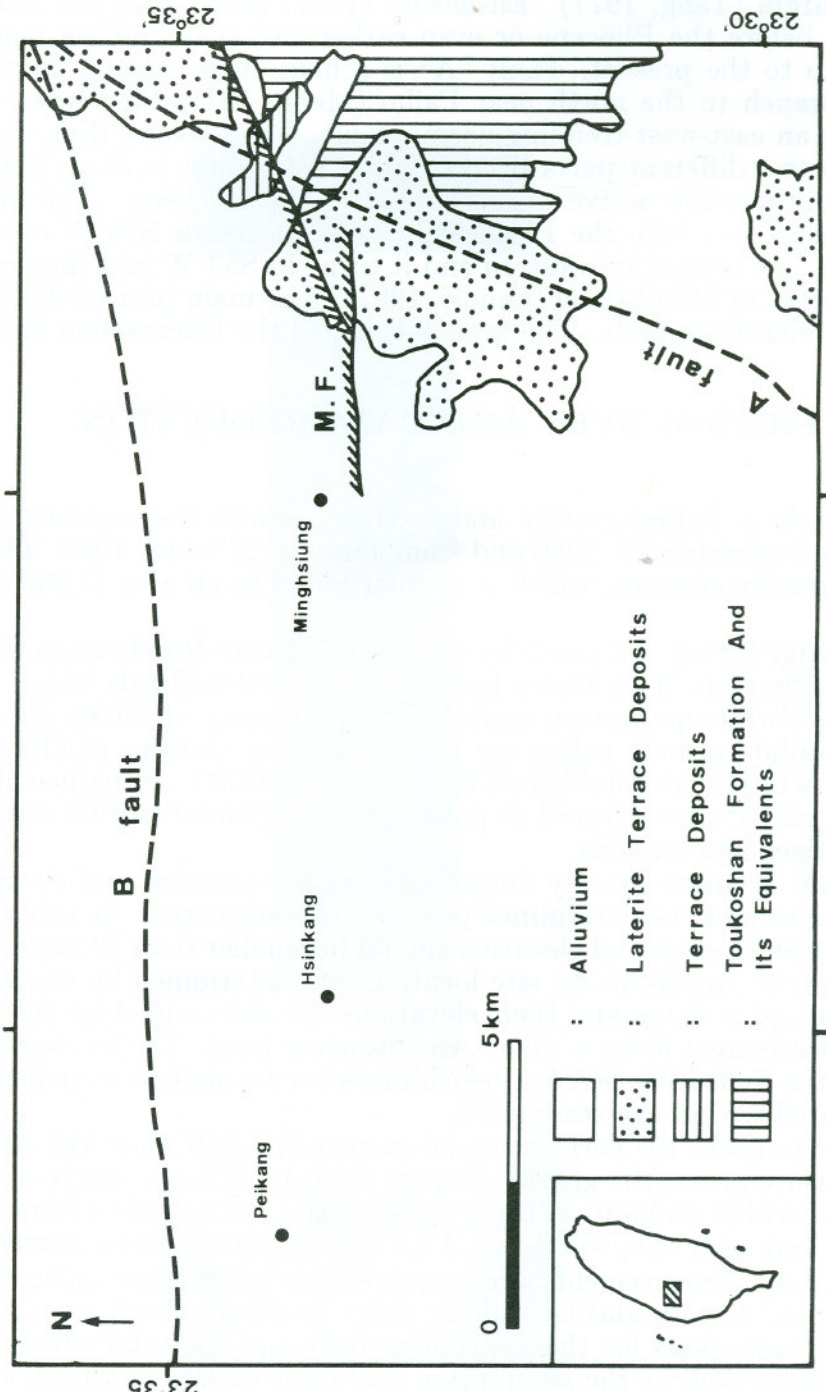

Fig. 1. Simplified geologic structure map of the Minghsiung-Peikang area(after Ho,1986).

Hinge fault", is regarded as the fault of the Peikang Basement High at the southern margin (Tang, 1977). Elishewitz (1961) noted that this fault was formed just before the Pliocene or even earlier and that faulting may have continued up to the present. Fault "A" is a high angle normal fault. This fault may branch to the north near Paiho (Meng, 1971; Elishewitz, 1961). Fault "B" is an east-west trending normal fault. The Peikang High is clearly divided into two different parts by this fault. According to Sun (1965) this fault was continuously active until the end of the Pliocene. The Meishan fault was associated with the 1906 earthquake. It trends S75°W over most of its length, but toward its western end it turns to S53°W and then extends nearly due west to Minghsiung (Omori, 1907). The main part of this fault is called the Meitzukeng fault. The branch is called the Chentsoliao fault.

FIELD SURVEY AND DATA REDUCTION

Field work including gravity and leveling surveys was conducted from August 5 to September 13, 1986 and from January 12 to 18, 1987. The total number of gravity stations, which were distributed in an area of 260 km^2 , is 592.

The gravity survey was made by using the LaCoste-Romberg model D-47 microgal gravimeter. This meter has a range of 200 milligals which can be reset for worldwide operations, and a reading accuracy of ±0.005 mgal. The observed absolute gravity values are tied to the base stations at Minghsiung and Chiayi, which were established by Yeh et al. (1979). To reduce observation error, gravity sites selected at points on solid ground and far away from tunnels, bridges and streams.

To ensure accurate gravity determination, the position and elevation of gravity stations must be determined precisely to some extent. In other words, the accuracy of location and elevation should be smaller than 12 meters and 5 cm, respectively. In this study, site locations are determined by using 1:5000 scale photographic maps and their elevations are determined by the closure leveling measurement using a Nikon AS automatic level. The leveling surveys are tied to the first order leveling bench marks or triangulation points which are distributed within the study area.

In order to make the corrections for instrument drift and tidal effects on gravity measurements, the gravity surveys are run on loops, where each loop is completed within an hour. A topographic description, made within a range of 25 m around each site, will be used for near-distance terrain correction.

The gravity measurements are corrected for instrument drift, tidal effects, elevation, terrain and latitude in order to obtain the Bouguer gravity anomalies. Corrections for the instrument drift and the tidal effects can be made reasonably well by the assumption that their variations within a period of about an hour are linear with time. Elevation correction includes free-air

and Bouguer corrections. Free-air corrections are made according to the expression for the vertical gradient -0.3086 mgal/m. Bouguer corrections are made by the formula for an infinite horizontal slab

$$\Delta g = 0.04185\rho H$$

where H is the height in meters relative to the datum level (e.g. sea level), ρ is the average density of strata between gravity site and datum, and Δg is the magnitude of Bouguer correction in mgal. In this study the datum is set at sea level. The average density of strata in the study area is assumed to be $2.0 gm/cm^3$ based on Hsieh and Hu's study (1972). Terrain corrections within the radius of 7 km from the gravity station are made principally by Hammer's method (1939). The latitude corrections are made according to the Geodetic Reference System Formula adopted by the International Union of Geodesy and Geophysics in 1967. The formula is

$$\gamma_0(gal) = 978.03185(1 + 0.005278895 sin^2\phi + 0.00002346 sin^4\phi)$$

where ϕ is the geographic latitude of site.

GRAVITY ANOMALY

After the corrections have been made, the Bouguer gravity anomaly of each site is obtained. Figs. 2 and 3 are the two- and three- dimensional Bouguer gravity anomaly maps. In general, contours of Bouguer anomalies trend in the NNW-SSE direction, except for some closed gravity low areas found near Hsinkang. The contour value ranges from +7.8 mgal to -7.5 mgal.

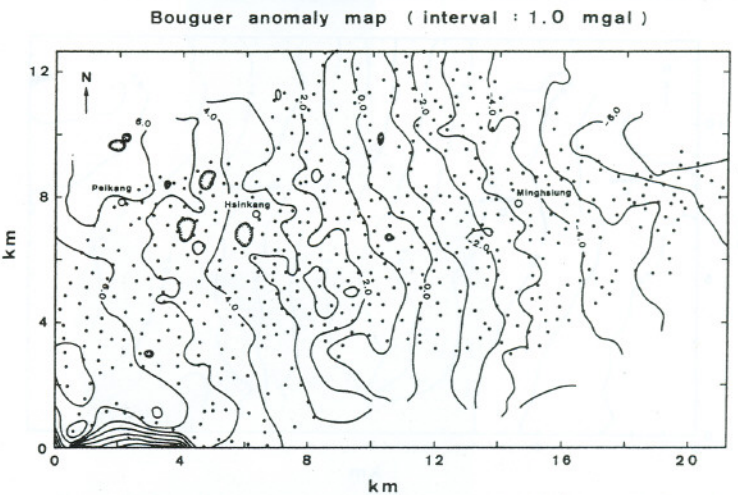

Fig. 2. Bouguer gravity anomaly map (contour interval: 1 mgal) and gravity stations (dots).

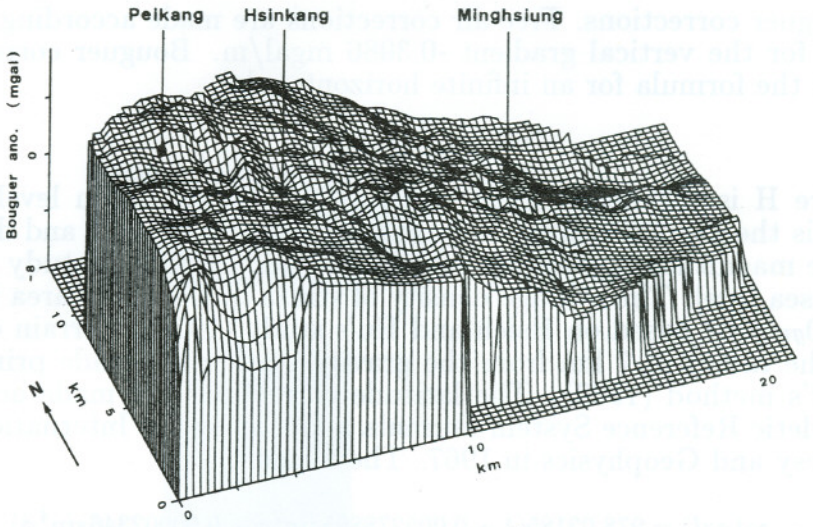

Fig. 3. Surface plot of Bouguer anomaly (rotated 20°W about Z-axis, tilted 40°).

The regional Bouguer gravity anomalies are determined by Griffin's formula (1949)

$$G_{reg} = (\sum_{i=1}^{8} G_i)/8$$

where G_i are the gravity values at the grid points with a distance of $\sqrt{5}$ grid intervals around the station. In this study, the grid interval is 200 meters. Fig. 4 shows the regional Bouguer gravity anomalies in two-dimensions. The contours distribute uniformly with a trend in the direction of N15°W. This phenomenon is similar to that obtained by Pan (1967).

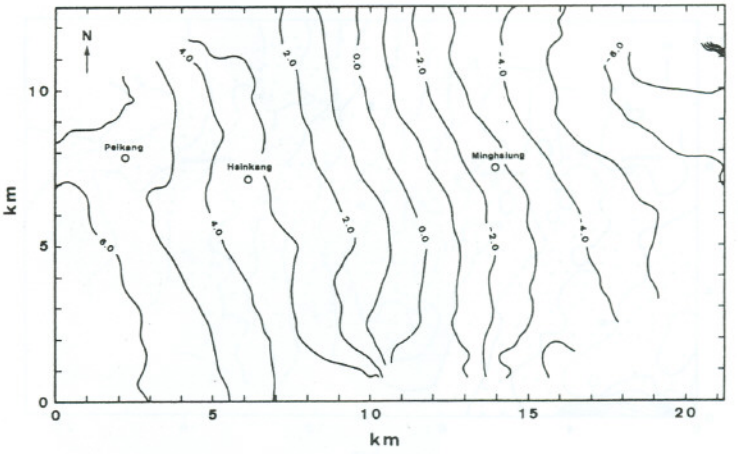

Fig. 4. Regional Bouguer gravity map (contour interval: 1 mgal).

Figs. 5 and 6 show the contours of residual gravity anomalies obtained by the formula

$$G_{res} = G_{obs} - G_{reg}$$

where G_{obs} is the observed gravity value and G_{reg} is the regional gravity value calculated by the formula mentioned above. There are several closed gravity

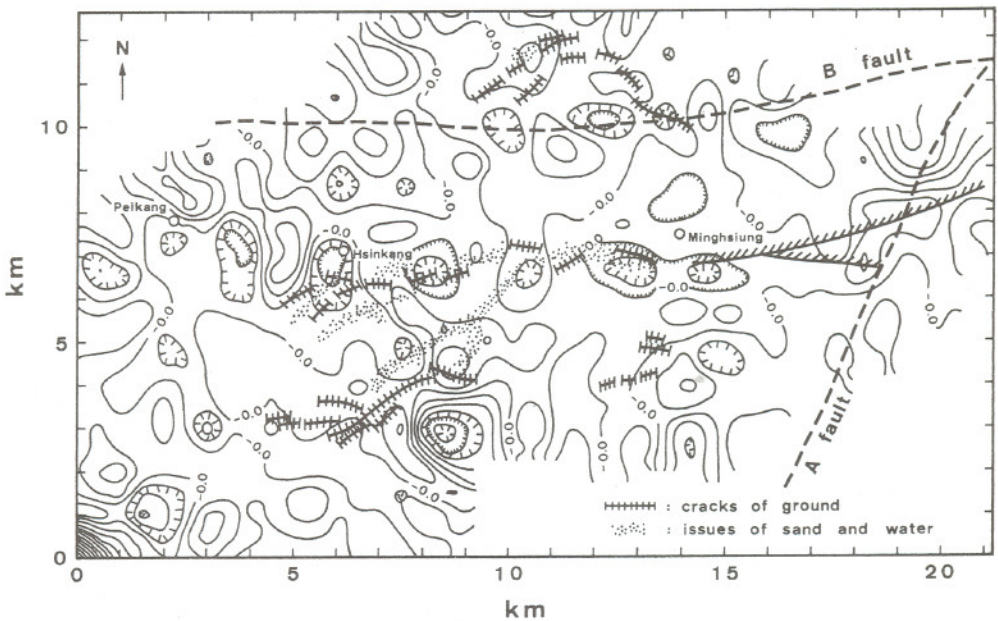

Fig. 5. Residual Bouguer gravity map (contour interval: 0.3 mgal).

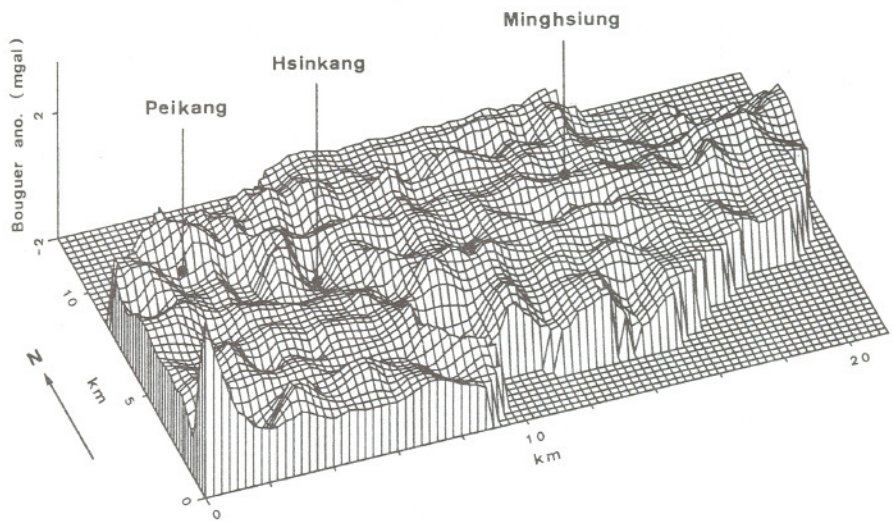

Fig. 6. Surface plot of Residual Bouguer anomaly (rotated 20°W about Z-axis, tilted 40°).

lows aligned with the locations where sand and water flowed out in 1906. This indicates that the anomalies may be caused by the fissures which occurred in 1906.

The second derivative Bouguer anomaly is calculated by the empirical formula of Henderson and Zietz (1949) and shown in Fig. 7. The formula is

$$\frac{\partial^2 G}{\partial^2 Z} = 2(3G_{obs} - 4\bar{G}_1 + \bar{G}_{\sqrt{2}})$$

where $\bar{G}_1$ is the mean value of gravity data around the station with a distance of 1 grid interval and $\bar{G}_{\sqrt{2}}$ is the mean value of gravity data around the station with a distance of $\sqrt{2}$ grid interval. Fig. 7 also reveals the gravity lows lining up consistently with the traces where sand and water flowed out in 1906.

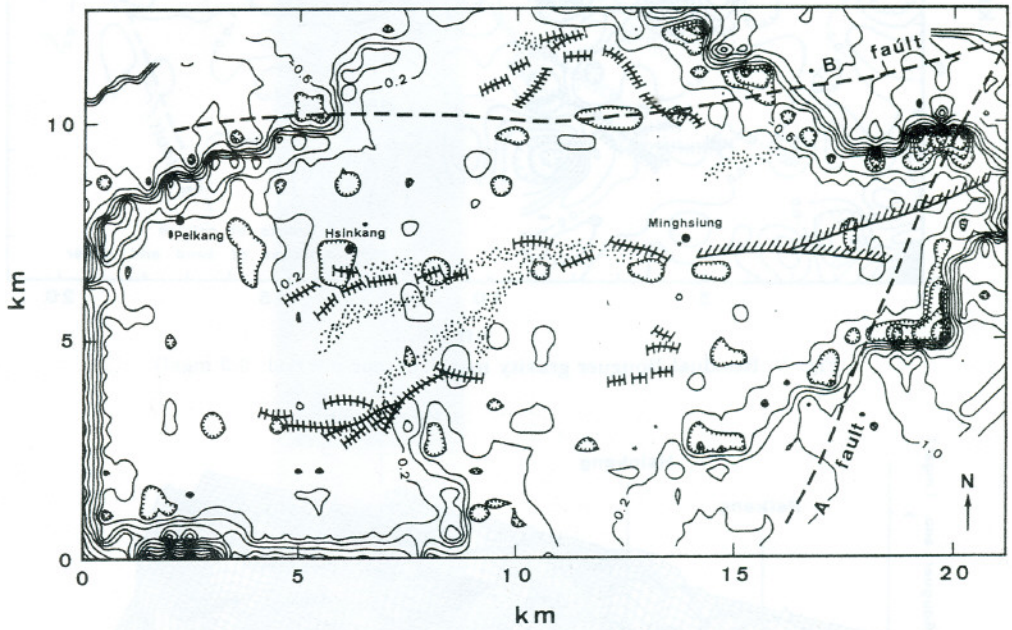

Fig. 7. Second derivative Bouguer anomaly map (contour interval: 0.4 mgal).

In general, the Bouguer anomaly values above the fault are distributed in the following patterns:

1. The contours distort suddenly. This effect is commonly shown by a strike-slip fault (Fig. 8). A greater displacement caused a more distinct distortion.
2. The contours abruptly become crowded or loose. Fig. 9 shows the dip-slip fault and the result caused by it. In this case, the larger vertical slide produced a greater gradient.

In nature, most faults are the combinations of strike-slip and dip-slip movement. The distribution pattern above the fault should be a combination of these two kinds of movement. Applying these two fundamental patterns,

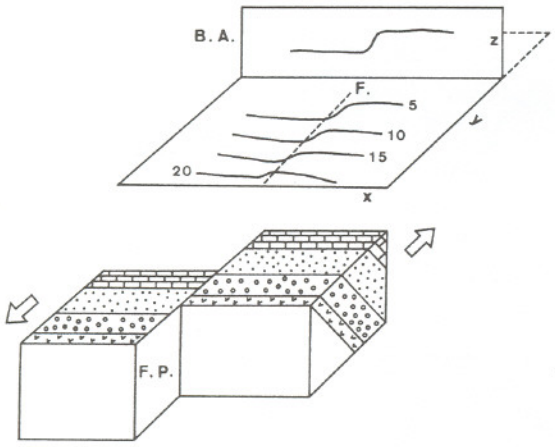

Fig. 8. Schematic diagram showing the gravity anomaly caused by a strike-slip fault.

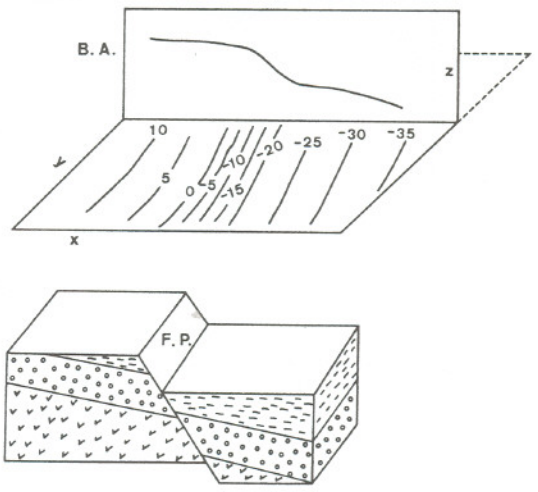

Fig. 9. Schematic diagram showing the gravity anomaly caused by a dip-slip fault.

we can roughly figure out the probable status of the faults. Hagiwara et al. (1986) used these ideas successfully to infer the status of active faults in the Nishi-Saitama area of Japan. In our study, the contours of Bouguer anomalies above the Meishan fault reveal some abrupt distortions and densenesses. This indicates that the Meishan fault is a fault with right-lateral and normal components. This is in agreement with the result of the surface geological surveys. From Minghsiung to Hsinkang there are also some distortions which indicates that the Meishan fault may extend to the west, as far as Hsinkang.

MODELING OF SUBSURFACE STRUCTURE

In order to model the subsurface structures, four gravity profiles roughly perpendicular to the fault are selected. The lengths of these profiles (AA', BB', CC', and DD' shown in Fig. 11) are from 10 to 12 km. The analytical gravitational field formula derived by Talwani et al. (1959) is used for the theoretical calculation. The observed and calculaed gravity values are matched as best as possible by trial and error.

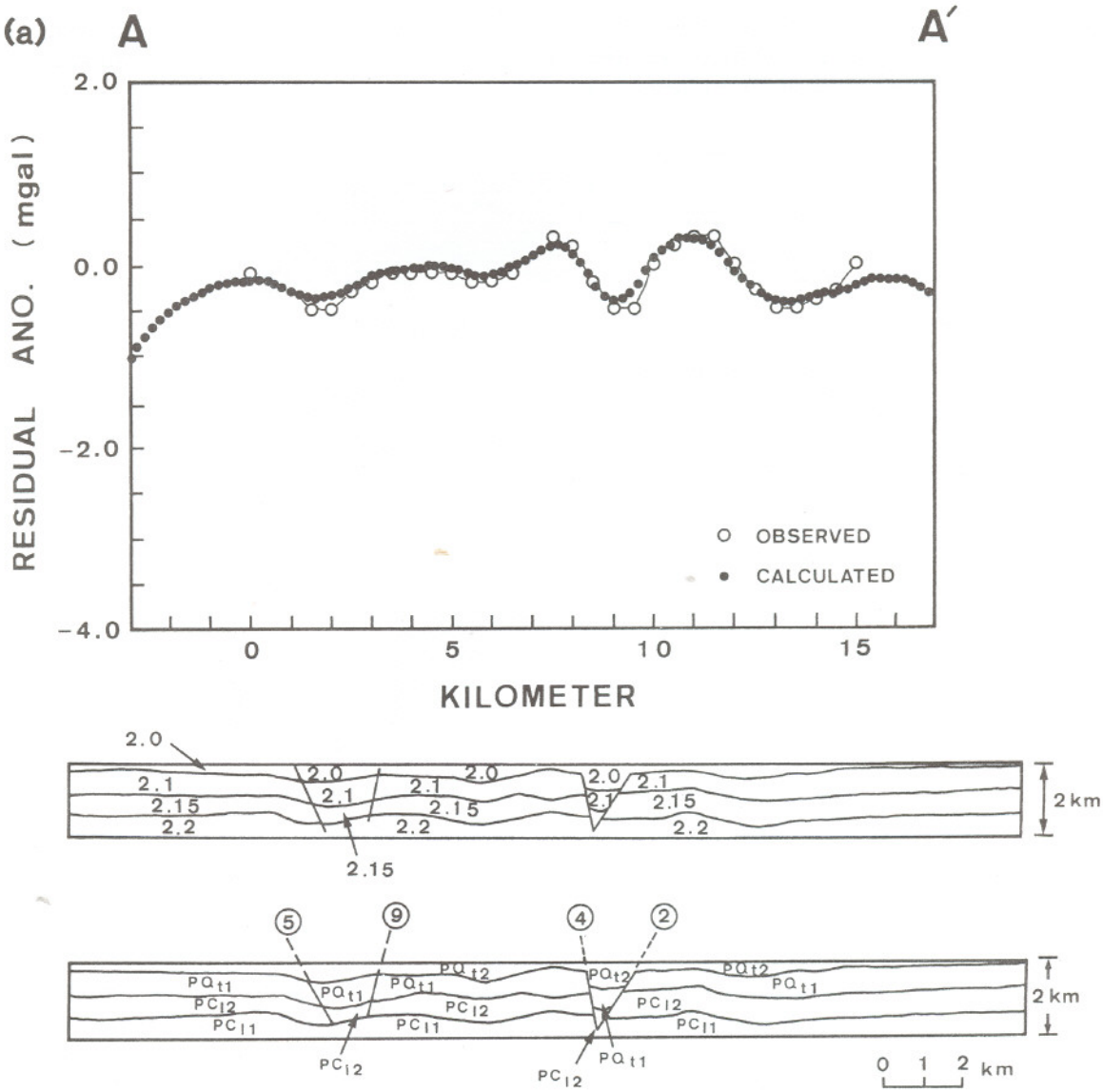

PQ$_{t2}$: Liushuang Formation
PQ$_{t1}$: Erhchungchi Formation
PC$_{12}$: Kanhsialiao Formation
PC$_{11}$: Liuchungchi Formation
PC$_{s}$: Yungshuichi Formation

②: Meitzukeng fault
③: Westward extension part of Meishan fault
④⑦⑧⑨: ? fault
⑤: `B´ fault

Fig. 10. Modeling results along the profiles (a) AA', (b) BB', (c) CC', and (d) DD'.

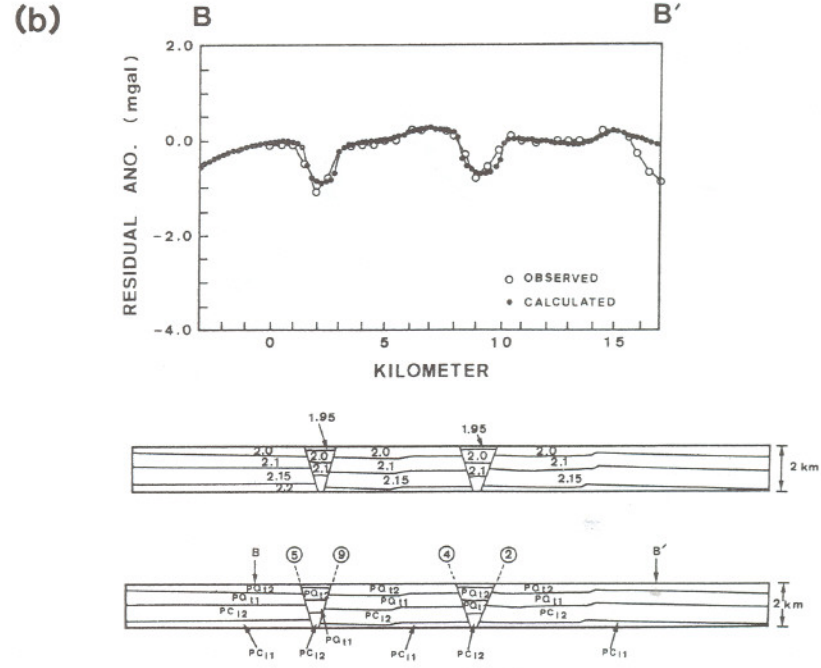

Fig. 10 (continued)

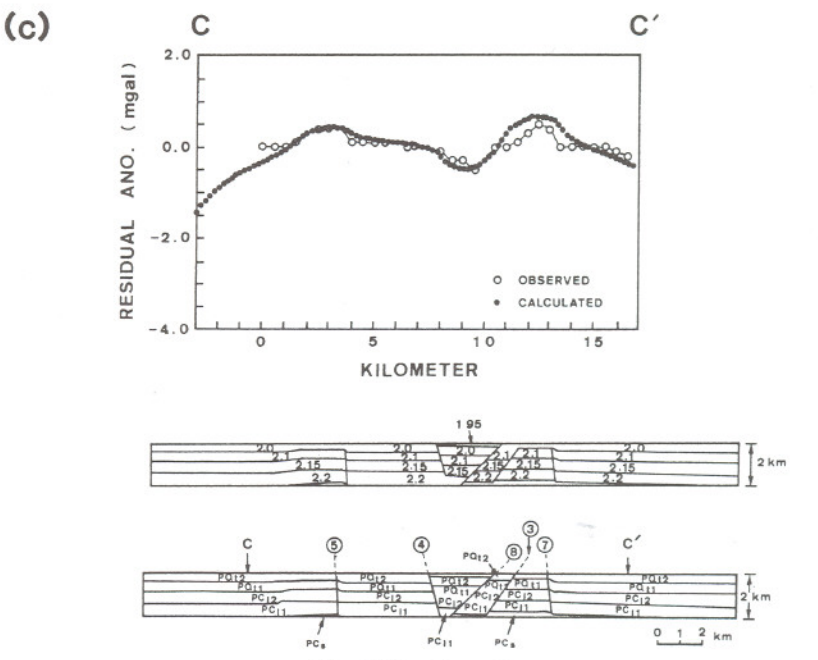

Fig. 10 (continued)

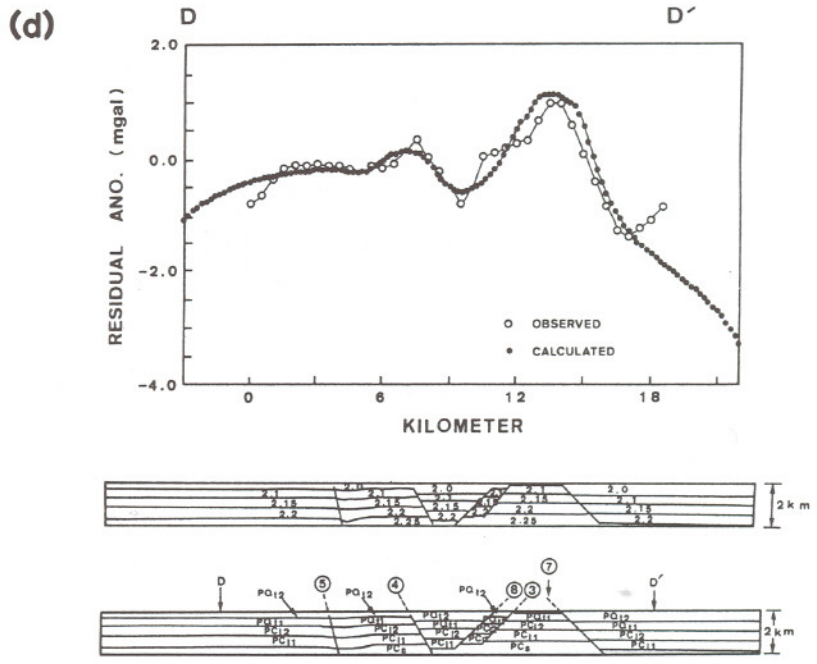

Fig. 10 (continued)

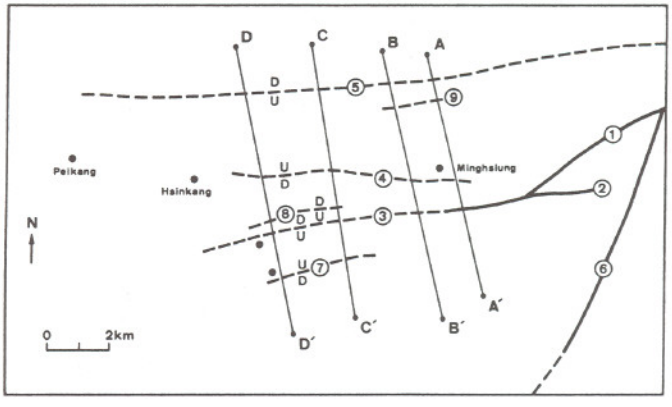

Fig. 11. Inferred geologic structures in the study area.

The optimum results of subsurface density distribution beneath the four profiles are shown in Fig. 10. In general, the calculated and observed gravity anomalies fit well. Some misfits may be due to the interpolations of two-dimensional contours into a one-dimensional profile, or the existence of anomalous bodies at very shallow depths. The inferred subsurface structures are also shown in the figure. Although the strata beneath this area are plain, most of them seem to dip to the south. The stratum thicken gradually from west to east. Based on the results of these four profiles and the studies of Hsiao (1970) and Kuan (1983), the subsurface geologic structures within the study area are inferred as shown in Fig. 11. The Meishan fault west to Minhsiung reveals the characteristics of a normal fault. Its vertical displacements vary from 50 to 200 meters. The apparent dip angles of this fault decrease from AA' to DD'. Fault "B" is a high angle normal fault dipping to the south. Its vertical displacements vary from 100 to 300 meters. Several faults are also modelled within the study area, such as fault 4, 7, 8, and 9 (shown in Fig. 11). All of them are normal faults. We believe that these faults resulted from the westward extension of the Meishan fault. The Meitzukeng fault, Chentsoliao fault and Fault "A", modelled by gravity data (Yeh et al.,1984), are also shown in Fig. 11.

CONCLUSIONS

A detailed gravity survey has been carried out in the Minghsiung-Peikang area in order to delineate the westward extension of the Meishan fault. In addition, Bouguer anomaly data of four profiles which run perpendicular to the Meishan fault are used for modeling the subsurface structures of this area. The results are summarized as follows:

(1) The distribution patterns of residual and second derivative Bouguer anomalies show some specific characteristics which are considered to beproduced by a fault. This indicates the possibility of the westward extension of the Meishan fault.

(2) The inferred subsurface structures show that the Meishan fault may extend at least 6 km westward from Minghsiung to Hsinkang. The west part of the Meishan fault dips at an angle of 60 to 80 degrees with a throw of 50 to 200 meters.

(3) Some normal faults exist in the study area. They possibly result from the westward extension of the Meishan fault.

ACKNOWLEDGEMENTS

The authors are grateful to their colleagues Messrs. Li-Wun Wang, and Wei-Chang Huang for participation in field work and assistance in data pro-

cessing. Thanks are also due to Ms. Huei-Fen Chiu for preparing the drawings. This study is supported by the National Science Council of the Republic of China Grant No. NSC76- 0414-P001-03B.

REFERENCES

Chang, Stanleys S.L.(1963) Regional stratigraphic study of Pleistocene and Upper Pliocene Formations in Chiayi and Hsinying Area, Taiwan:*Petrol. Geol. Taiwan* **2**, 65-86.

——— (1964) Regional stratigraphic study of the Lower Pliocene and Upper Miocene Formations in northern Taiwan:*Petrol. Geol. Taiwan* **3**, 1-20.

Elishewitz , B. (1961) West-Central coast plane region of Taiwan: *unpublished report, CPC file.*

Griffin W.R. (1949) Residual gravity in theory and practise:*In "Applied Geophysics", ed. by Telford, W.M. et al.*, 860 p.

Hagiwara Y., I. Murata, H. Tajima, K. Nagasawa, and S. Izutuya (1986) Gravity study of active faults- detection of the 1931 Nishi-saitama Earthquake fault-: *Bull. Earthq. Res. Inst. Univ. Tokyo*,**61**, 563-586.

Hammer, S. (1939) Terrain correction for gravimeter stations: *In "Applied Geophysics", ed by Telford W.M. et al.*, 860 p.

Henderson, R.G. and Zietz, I. (1949) The computation of second vertical derivatives of geomagnetic fields:*In "Applied Geophysics", ed. by Telford, W.M. et al.*, 860 p.

Ho, C.S. (1975) An introduction to geology of Taiwan-explanatory text of the geologic map of Taiwan: *The Ministry of Economic Affairs, Taipei, Taiwan, R.O.C.*, 153 p.

Hsiao, P.T. (1970) Seismic study of the area between the Coastal Plain and the Foothills, Chiayi, Taiwan:*Petrol. Geol. Taiwan* **7**, 47-52.

Hsieh, S.H. and Hu, C.C. (1972) Gravimetric and magnetic studies of Taiwan:*Petrol. Geol. Taiwan* **10**, 283-321.

Hsu, M.T. (1980) Earthquake catalogues in Taiwan(From 1964 to 1979), *Earthq. Eng. Res. Cent., National Taiwan Univ.*, 77 p.

Kuan, M.Y. (1983) Subsurface geology of the southwestern plain of Taiwan:*Taiwan Mining Industry*, **36, 1**, 80-84, (in Chinese).

Meng, C.Y. (1971) A conception of the evolution of the Island of Taiwan and its bearing on the development of the Western Neogene Sedimentary basins:*Petrol. Geol. Taiwan*,**9**, 241-258.

Omori, F. (1907) Preliminary note on the Formosa earthquake of March 17, 1906, *Imp. Earthquake Inves. Comm. Bull.*,**2**, 53-69.

Pan, Y.S. (1967) Interpretation and seismic coordination of the Bouguer gravity anomalies over West-Central Taiwan:*Petrol. Geol. Taiwan* **5**, 99-115.

Sun, S.C. (1965) Geology and petroleum potentialities of the Chingshui-Yuanlin area, Taiwan: *Petrol. Geol. Taiwan*, **4**, 161-173.

Talwani, M., Worzel, J.L. and Landisman, M. (1959) Rapid gravity computations for the two-dimensional bodies with application to the Mendocino submarine fracture zone:*J. Geophys. Res.* **64**, 49-59.

Tang, C.H.(1977) Late Miocene erosional unconformity on the subsurface Peikang High beneath the Chiayi-Yunlin coastal plain,*Taiwan. Mem. Geol. Soc. China*, **no. 2**, 155-168.

Yeh, Y.H., S.K. Huang, Y.H. Tzou, Y.B. Tsai, and Y.S. Wu (1979) Repeat gravity measurements in Taiwan: *Open File Report, Inst. Earth Sci., Academia Sinica* 198 p. (in Chinese).

———, Wang, W.H., Yen, H.Y. and Tsai, Y.B. (1984) Subsurface structures in the Minghsiung-Meishan area, southwestern Taiwan from gravity anomaly data: *Bull. Inst. Earth Sci., Academia Sinica* 4, 101-116.